The impact of bearing conditions on the stability behavior of cold-formed steel stud assemblies

Abbas Joorabchian[1], Zhanjie Li [2], Kara D. Peterman [3]

Abstract
The objective of this study is to explore the stability response of cold-formed steel stud assemblies (i.e., stud and track) with partial bearing conditions. Studs bearing under partial bearing conditions (i.e., not fully bearing on a concrete slab) may result in reduced axial capacities. Currently, behavior of these systems due to member instability is not well-understood, and cold-formed steel design specifications provide no guidance. This study provides an integral experimental and numerical investigation of the stability response of the studs under partial bearing conditions in order to quantify the reduction of their axial capacities. A variety of stud sections with different geometries and thicknesses and a variety of partial bearing conditions are considered in this study by parametrically varying edge (i.e., where the steel stud assembly is close to the concrete slab edge) and overhang (i.e., steel stud assembly is outside the edge) distances. The results of this study will be used to develop design guidelines for stud wall assembly under non-uniform bearing conditions.

1. Introduction
Cold-formed steel (CFS) members are utilized widely in light framed constructions for structural (load bearing) and nonstructural members (Joorabchian et al. 2018). CFS studs generally forming the walls of such structures are commonly capped in two horizontal tracks at the top and bottom (Figure 1) (Peterman and Schafer 2014; Vieira et al. 2011).
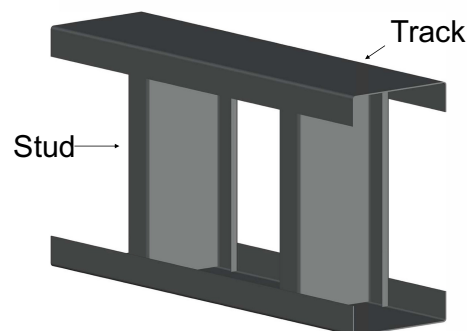

Figure 1: Stud-track assemblies (Joorabchian et al. 2018)

[1] PhD Candidate, University of Massachusetts Amherst, <ajoorabchian@umass.edu>
[2] Assistant Professor, The SUNY polytechnic institute, < zhanjie.li@sunyit.edu >
[3] Assistant Professor, University of Massachusetts Amherst, <kdpeterman@umass.edu>

The walls are typically placed on the concrete slab floors, and the exterior walls may have some distance or overhang from the slab edge, which results in a non-uniform bearing condition and stress distribution on the stud end. Studs bearing under these situations will have reduced axial capacity, and current practice does not recognize a difference in the axial capacity or behavior due to partial end supports. Furthermore, design codes such as the North American Specification of the American Iron and Steel Institute (AISI) do not provide any guidance on the calculation of this reduced axial capacity in AISI S100-16 and S240-15.

A wealth of data exists on the performance of axially-compressed studs and stud assemblies, but in previous work, the concrete slabs are assumed to provide rigid uniform support resulting in a uniform stress distribution on the stud end (Peterman and Schafer 2014; Vieira et. al 2011; Vieira and Schafer 2011; Georgieva et al. 2012; Li et al. 2014; Ye et al. 2016 Liu and Zhou 2017; Liao et al. 2017; Fratamico et al. 2016). These works further do not capture the spalling or crushing of the concrete slab, which only intensifies the non-uniform condition at the stud end and may ultimately reduce contact.

Bae (2006) investigated the axial strength of CFS walls on concrete slabs. The research program was experimental in nature, and primarily examined the effect of wall stud configurations on the performance of the system. Single stud columns, single stud walls, back-to-back stud columns, and back-to-back stud walls were tested on an 89 mm concrete slab intended to simulate typical residential floor systems. Specimens were cut to 51 mm in height to force failure into the slab, rather than buckling of the stud. FEM was conducted to determine the stress distribution in the concrete slab, through the track section. The work demonstrated that edge distance did impact system bearing strength, and results were used to develop a method of determining the bearing area for the stud-track assembly on concrete slabs, which accurately predicted experimental results. It also demonstrated the inadequacy and inapplicability of the bearing provisions in ACI 318-05 (Building Code Requirements for Reinforced Concrete) for CFS wall systems. While this study expanded the state of knowledge for how stud assemblies interact with concrete foundations, it was limited in scope to one stud size and one stud height which in turn restricted failure modes to the slab and did not permit local buckling of the stud. Polyzois and Fox (2001) did a research at the University of Manitoba supporting a reduction in stud axial capacity due to stud distance from slab edge. The experimental program undertaken by the authors included stud assemblies located 8" from the stud edge, and assemblies located at the stud edge. The studs were sized such that they were permitted to buckle locally, unlike in the Bae et al (2006) work. Assemblies located at 8" from the slab edge developed their local buckling capacity while those installed on the edge were hindered by concrete spalling and cracking – their axial compressive strength decreased by 15-25%, due to the reduction in bearing area, and loss of a uniform stress distribution. The work examined one stud-track assembly and did not consider intermediate edge distances. Neither of these studies explore a range of studs and track assemblies.

The aim of this research project is to quantify the impact of the concrete slab as a flexible or semi-rigid support and the edge distance on the axial capacity of stud-track assemblies. This paper starts with describing the statement of the work and then an explanation about the test setup. Results and discussion follow.

2. Statement of Work

The tests reported here are a part of a comprehensive research project the aim of which is to characterize experimentally and computationally the effect of stud bearing on concrete slabs, examining overhang distance, edge distance, section geometry, and various assembly configurations. Table 1 demonstrates which specimen configuration are to be included in the experimental test matrix. In order to validate the experimental results, all the configurations will be modeled in ABAQUS. In this paper, only the behavior of 54 mil (1.37 mm) studs with flanges of 1.62 and 3 inch (4.11 and 7.62 cm) long are examined.

Table 1: Experimental test matrix

Stud	Track	Phase 2: Full Bearing Condition	Phase 3: Edge Condition	Phase 4: Effect of Overhang
600S162-33	600T162-33	Center of slab/Full bearing (edge distance>6" (15.25 cm))	at slab edge 1" (25.4 mm) from slab edge 0.5" (12.7 mm) from slab edge 0.125" (3.175 mm) from slab edge	0.5" (12.7 mm) overhang 1" (25.4 mm) overhang
600S162-54	600T162-54	Center of slab/Full bearing (edge distance>6" (15.25 cm))	at slab edge 1" (25.4 mm) from slab edge 0.5" (12.7 mm) from slab edge 0.125" (3.175 mm) from slab edge	0.5" (12.7 mm) overhang 1" (25.4 mm) overhang
600S162-97	600T162-54	Center of slab/Full bearing (edge distance>6" (15.25 cm))	at slab edge 1" (25.4 mm) from slab edge 0.5" (12.7 mm) from slab edge 0.125" (3.175 mm) from slab edge	0.5" (12.7 mm) overhang 1" (25.4 mm) overhang

Stud		Phase 5: Effect of Flange Width
600S300-54	600T162-54	at slab edge 1" (25.4 mm) from slab edge 0.5" (12.7 mm) from slab edge

*Phase 1 is not included in this table and it is for the rigid bearing condition

3. Test Setup and Instrumentation

The test program occurred at the Gunness structural laboratory of University of Massachusetts Amherst. The experimental tests were performed on a structural testing frame consisting of six built-up beams. A 110 kips (489 kN) MTS actuator was utilized to apply the axial load (Figure 2). Load and displacements were measured via the crosshead load cell and a built-in LVDT respectively. WinDaq software was used for data acquisition. There were two types of experimental test: the tests with concrete slabs and those ones without slab the schematic views of which are shown in Figure 3. The test without concrete slab was considered for rigid bearing condition. In order to provide that condition, a built-up beam consisting of two 8×1 inch (20.32×2.54 cm) and one 4×1 inch (10.16×2.54 cm) was designed and placed under the stud assembly. To prevent any possible uplift of the concrete slabs in the conditions which the stud assembly is fastened near to the slab edge, an L 8×6×1 angle was designed and connected to the test rig beams by two L 8×6×1 angles (Figure 2).
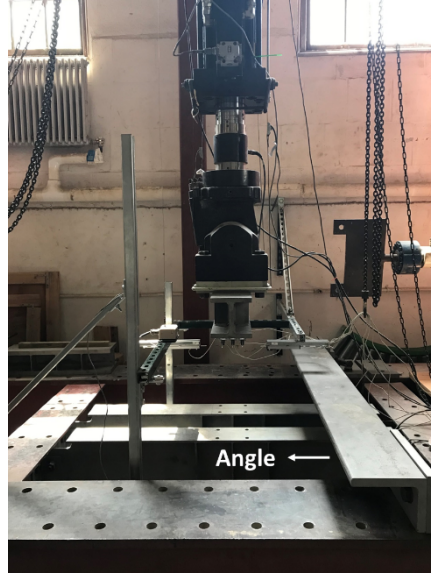
Figure 2: The test rig of Gunness structural laboratory (University of Massachusetts Amherst)

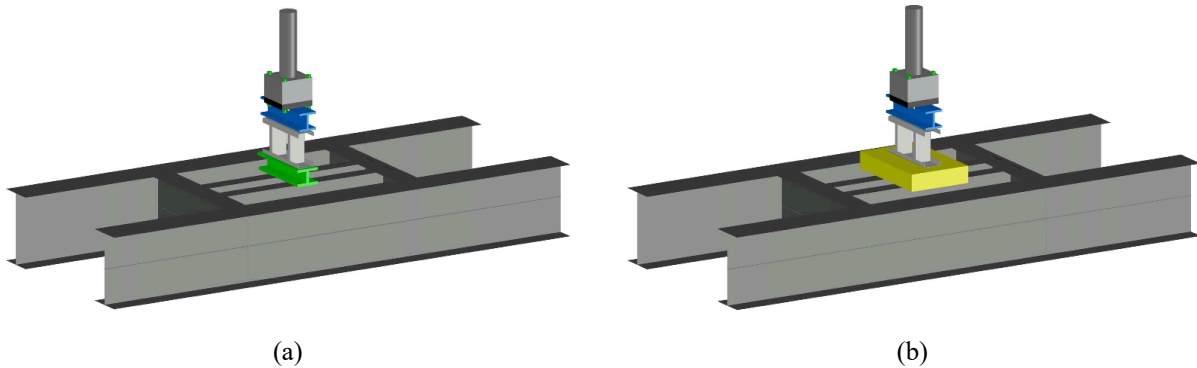(a)   (b)

Figure 3: The schematic views of the tests; (a) tests with no slab, (b) tests with slab

The test specimens included two studs, 12 inches (30.48 cm) long and 12 inches (30.48 cm) apart, capped in two horizontal 24 inches (60.96 cm) long tracks at the top and bottom. In total, 11 stud-track assembly were prepared. 54 mil (1.37 mm) studs fastened to 54 mil (1.37 mm) tracks with #12 steel-to-steel hex washer head screws. For this part of the project, ten 4 ksi (27.58 MPa) reinforced concrete slabs with dimensions of 22×34×6 inch (30.48×86.36×15.24 cm) were poured. Two layers of rebar mesh (W4 6×6) were utilized to meet ACI 318-14 minimum requirements. According to ACI 318-14, concrete cover was considered 3/4 inch (1.9 cm)(Figure 4).

The tested edge distances includes at the middle of slab (11 inch or 27.94 cm), at edge, 1, 0.5, and 0.125 inch (25.4, 12.7, and 3.175 mm) from edge. Moreover, overhang distances includes 1/2 and 1 inch (12.7 and 25.4 mm). To attach stud-track systems to concrete slabs and provide mentioned distances, three single concrete nails with plastic washer were utilized. The size of nails was 0.157 inch in diameter and 1-1/16 inch in length (4×27 mm) and a powder actuated tool was deployed for fastening the single nails six inches (15.24 cm) apart.

In order to capture the deformation of the studs during the tests, five transducers, two for the flanges and three for the stud web, were utilized. To install and place the sensors at the middle of the studs, a frame built from slotted strut channels was constructed. Since the sensor frame was

fabricated from slotted strut channels, the sensors height was adjustable; hence, they were placed at the middle of a stud height. Figure 4 shows the sensor frame as well as the placement of the transducers. Besides mentioned transducers, to record the deflection of top beam holding the actuator and the beams underneath of concrete slabs (or the rigid beam for the test with no slab), two string potentiometers were utilized. The first one was connected to the top beam and the frame holding the transducers and the second one was connected to one of the rig beams and lab floor.
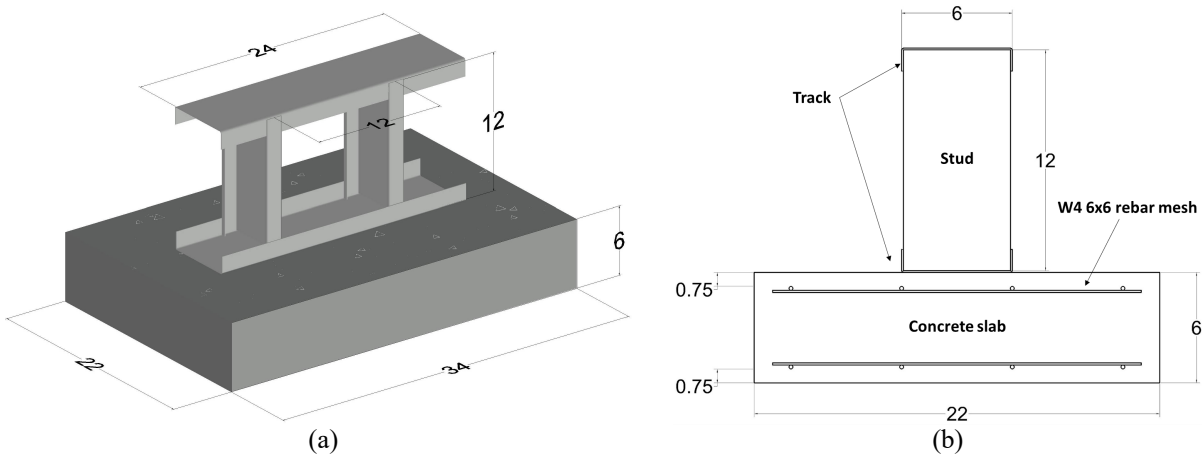

Figure 4: Stud-track assembly and concrete slab configuration (all units are inches); (a) 3D view, (b) side view
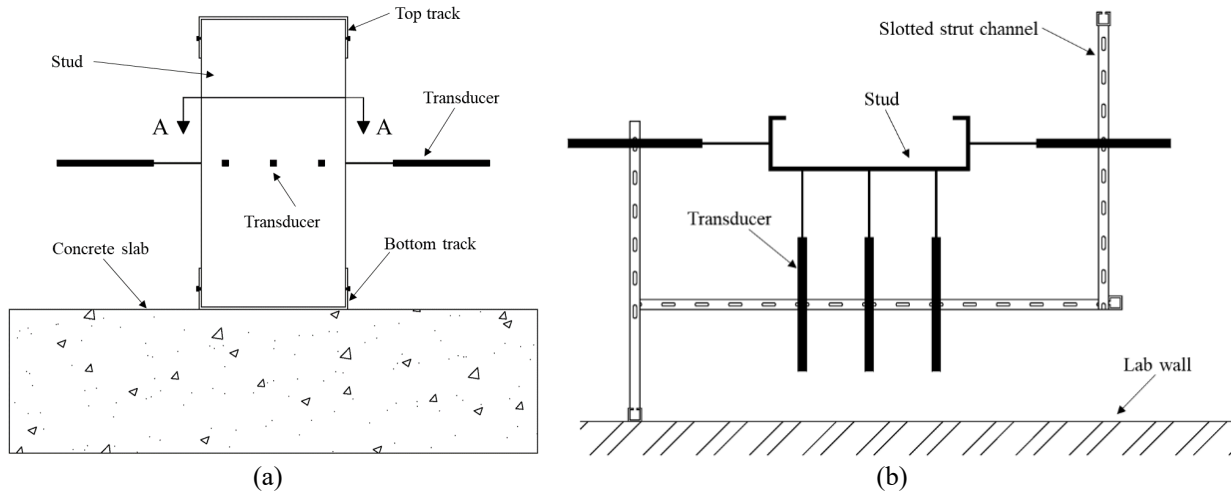

Figure 5: The sensor frame and placement of the transducers; (a) side view, (b) top view (section A-A)

The tests are denominated in such a way identifying both section name and bearing condition. Figure 6 demonstrate how the tests are named.
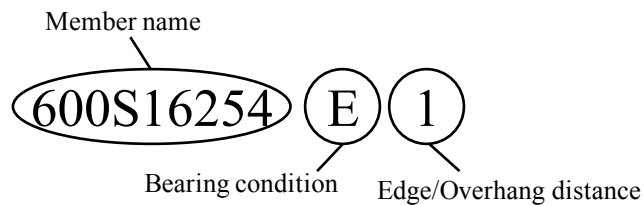

Figure 6: Experimental nomenclature

The members discussed in this research project are 600S162-54 and 600S300-54; the numbers 1, 05, and 0125 in the test names representing 1, 0.5, and 0.125 inch (25.4, 12.7, and 3.175 mm) to the slab edge and finally, the symbols used for each bearing condition are shown in Table 2.

Table 2: Bearing conditions and their symbols in the test names

Bearing Condition	Symbol in the test name
Full/Rigid	F
Center of slab/ Full bearing	C
Close to the edge	E
Overhang	O

For the rigid bearing condition, the stud assembly was clamped to the rigid beam using C-clamps. These clamps were adequate for pure axial load case as the load is centric to the centroid of the stud and no out of plane force were presented. As mentioned before, the compression loading was applied using a 110 kips (489 kN) MTS actuator and a displacement-controlled load equal to 0.01 in/min (0.254 mm/min) was applied monastically until failure; the compression load was distributed to the assembly via a built-up beam installed under the actuator. For both types of the tests, the top track was clamped to that beam to prevent any displacement and sliding.

4. Experimental results

It was expected a combination of local and distortional buckling took place in the studs, and the test observations proved this hypothesis. Example of deformed shapes of 600S162-54 stud assemblies under the peak loads are shown in Figure 7.
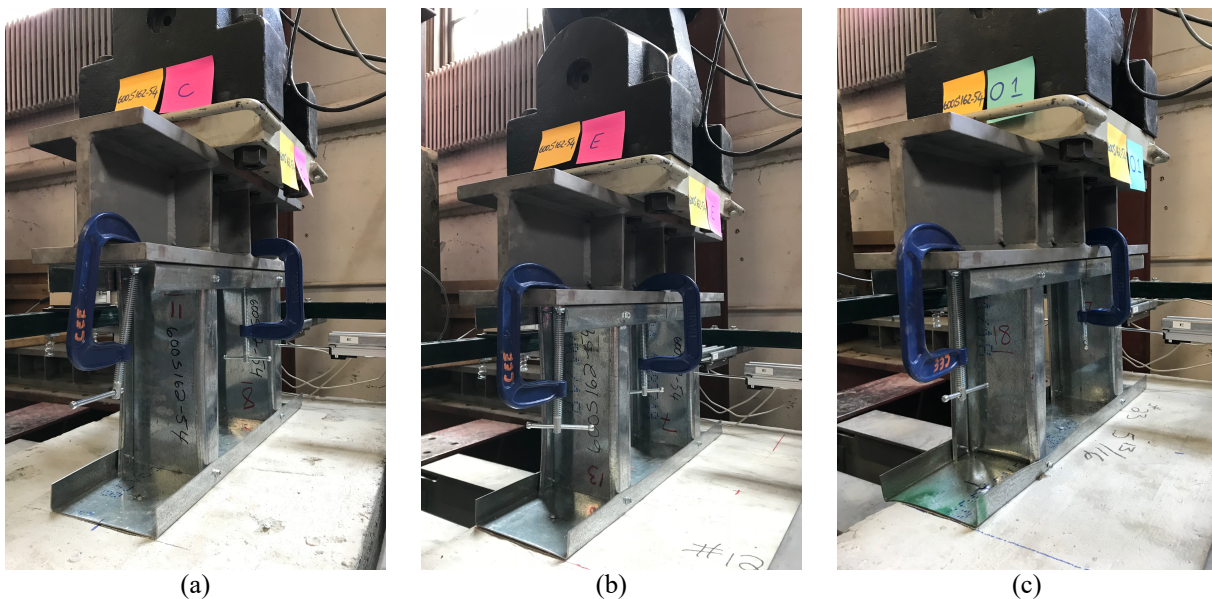

| (a) | (b) | (c) |

Figure 7: Deformed 600S162-54 assemblies under the peak loads; (a) full bearing (at the center), (b) at the edge, (c) 1 inch (2.54 cm) overhang

The primary test results of all 11 tests are summarized in Table 3. The axial capacities of the assemblies under both rigid and full (center of slab) bearing conditions are almost same and is 30.64 kips (136.28 kN) which is the highest peak load. It indicates when the stud-track assembly has enough distance from the edge of concrete slab, in this case 8 inches (20.32 cm), the slab can

keep the stress distribution uniform. However, as the assembly get closer to the edge and even outside the edge, the impact of bearing condition is more significant and the concrete slab acts as a flexible support causing a non-uniform stress distribution. For instance, when the assembly was one inch away from the edge, the axial capacity is reduced by 10%, but when it was located at the edge, it is decreased 15%, which shows how the non-uniform stress distribution can impact the axial strength of wall assemblies. Moreover, the non-uniform stress distribution is detrimental to the system stiffness as well.

Table 3: Test results for 54 mil sections

Test Name	Bearing Condition	P_{max}	$\triangle$ at P_{max}	k_i	1-P_{max_r} / P_{max}
		kips (kN)	inches (mm)	kips/in (kN/mm)	%
600S16254F	Rigid	30.64 (136.28)	0.186 (4.71)	411 (71.9)	-
600S16254C	Full bearing	30.66 (136.39)	0.225 (5.72)	382 (67.0)	-
600S16254E1	1" to edge	27.67 (123.07)	0.278 (7.06)	249 (43.7)	10%
600S16254E05	0.5" to edge	28.63 (127.33)	0.247 (6.27)	282 (49.4)	7%
600S16254E0125	0.125" to edge	26.44 (117.61)	0.228 (5.80)	283 (49.5)	14%
600S16254E	at the edge	25.97 (115.51)	0.257 (6.52)	291 (51.0)	15%
600S16254O05	0.5" overhang	24.17 (107.52)	0.234 (5.96)	226 (39.7)	21%
600S16254O1	1" overhang	20.03 (89.09)	0.287 (7.29)	196 (34.4)	35%
600S30054E	at the edge	25.62 (113.94)	0.293 (7.45)	180 (31.6)	-
600S30054O05	0.5" overhang	21.05 (93.65)	0.246 (6.24)	201 (35.2)	-
600S30054O1	1" overhang	16.73 (74.44)	0.297 (7.55)	119 (20.8)	-

The load-displacement curves of all the tests are shown in Figure 8.

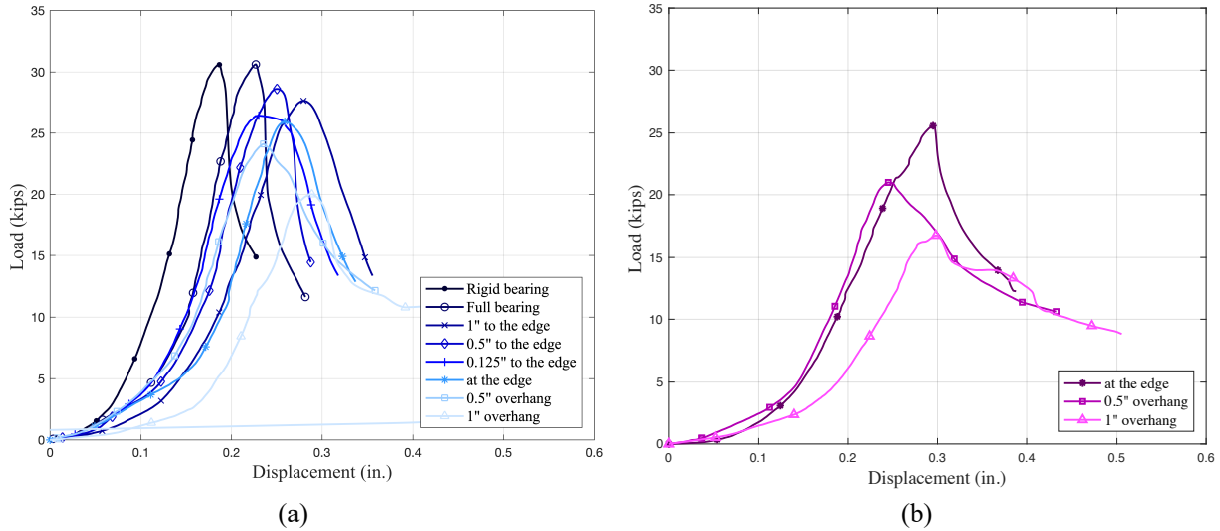(a)   (b)

Figure 8: Load vs. displacement curves of the tests; (a) 600S162-54 stud assemblies, (b) 600S300-54 stud assemblies

Figure 8 shows again the impact of bearing conditions on the axial capacity of the stud assemblies. In the overhang conditions, in addition to the impact of stress distribution, the reduced section causes sever reduction in the axial strength, for example, for the 600S162-54 assemblies, for one inch (25.4 mm) overhang, it is reduced 35% in comparison with rigid end support. This phenomenon is verifiable when the flange length is increased from 1.62 inch (4.11 cm) to 3 inches (7.62 cm); the behavior of these assemblies is shown in Figure 9.

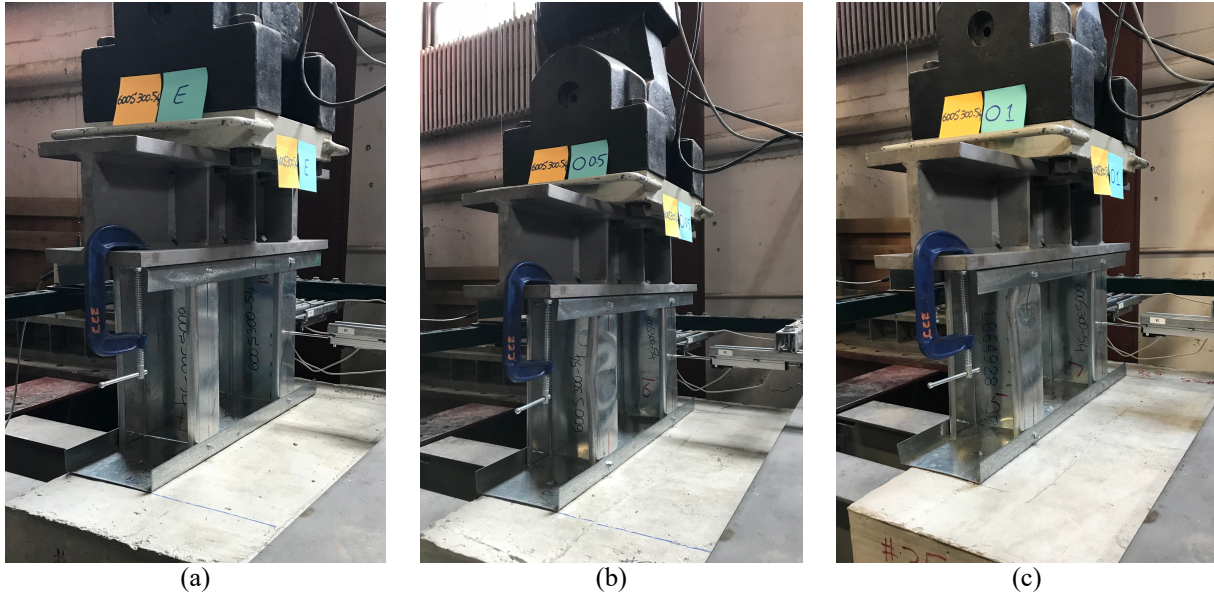<div align="center">(a)   (b)   (c)</div>

Figure 9: Deformed 600S300-54 assemblies under the peak loads; (a) at the edge (b) 0.5 inch overhang (1.27 cm), (c) 1 inch (2.54 cm) overhang

5. Comparing with Finite Strip Analysis Results

As a preliminary comparison between the experimental results and the computational ones, the sections are modeled in CUFSM (Schafer and Ádány 2006; Li and Schafer 2010) for elastic buckling analysis (Table 4). It can be considered as a mean of predicting the buckling response of the stud assemblies. CFS members are not perfect and their dimensions and material properties are different from the nominal properties and may impact the strength of members (Joorabchian and Peterman 2018), so for modeling the sections, the average of their thickness measured in the lab (0.0584 inch or 1.48 mm) was utilized. For 600S162-54 members, in total, 37 nodes and 36 elements were used. And for the 600S162-300 ones, 39 nodes and 38 elements were used. The modulus of elasticity for material properties was considered 29500 ksi (203 GPa). Simple-simple condition are assumed for the boundary condition. For all the conditions except the overhangs, it was assumed they all have the same end support since they are placed on either a concrete slab or a rigid beam, which means the entire of the cross section can carry the axial load. The stress was assumed uniform in the model, though, based on the previous experimental tests, this would not be the case when the assembly was close to the edge. Nonetheless, the modeling exercise herein by assuming uniform follows the current design practice reflected by the current design specifications. However, the reduced sections (portion of cross section which directly bears on slab) were modeled for overhang conditions.

Table 4 shows the buckling strength of assemblies based on the finite strip analysis. Moreover, the buckling mode and the contribution of each mode is determined. The buckling load for all of the conditions is a combination of local and distortional buckling but the domination of distortional buckling is evident. These buckling strengths do not match the axial capacities of the wall assembly from the test but serve as a good strength indicator that can be used in design strength predication. From the experiments, the axial capacity of rigid bearing condition, the most similar boundary condition to the modeled sections in CUFSM, is 30.64 kips (136.28 kN) which has 17% difference to the buckling strength in the Table 4. Meanwhile, this indicates that the wall assembly failed in distortional buckling demonstrated a moderate post-buckling reserve.

Table 4: Finite strip analysis results

Test Name	Bearing Condition	CUFSM	buckling mode	
			Local	Distortional
		kips (kN)	%	%
600S16254F	Rigid	25.43 (113.12)	13.7	83.4
600S16254C	Full bearing	25.43 (113.12)	13.7	83.4
600S16254E1	1" to edge	25.43 (113.12)	13.7	83.4
600S16254E05	0.5" to edge	25.43 (113.12)	13.7	83.4
600S16254E0125	0.125" to edge	25.43 (113.12)	13.7	83.4
600S16254E	at the edge	25.43 (113.12)	13.7	83.4
600S16254O05	0.5" overhang	20.48 (91.09)	15.3	81.7
600S16254O1	1" overhang	19.31 (85.89)	16.5	80.6
600S30054E	at the edge	34.21 (152.17)	23.3	75.3
600S30054O05	0.5" overhang	24.59 (109.40)	25.7	73.2
600S30054O1	1" overhang	23.23 (103.34)	27.5	71.5

6. Comparison with AISI S100-16 strength prediction

Another mean for comparing the experimental and numerical results is the methods provided in AISI S100-16. For the members subject to the pure compression, the prediction can be performed in accordance with Eq. 1.

$$P_u \leq \varphi_c P_n \qquad (1)$$

Where, P_u is required compression strength (demand), P_n is nominal compression strength or capacity, and φ_c is a factor for compression converting the nominal strength to available capacity. Based on the AISI S100-16, this expression can be used for all the conditions under the compression except overhang. For the overhang conditions, a part of the stud-track system is out of the concrete slab which leads to an eccentric axial load. The eccentricities are calculated in Table 5. In these cases, the systems are subject to a combination of compression and flexure; hence, the allowable strength shall be determined by employing Eq. 2.

Table 5: Calculated eccentricities for overhang conditions

Section	Overhang distance	e
	in. (mm)	in. (mm)
600S162-54	0.5 (12.7)	0.0294 (0.75)
	1 (25.4)	0.0668 (1.70)
600S300-54	0.5 (12.7)	0.0306 (0.78)
	1 (25.4)	0.0593 (1.51)

$$\frac{\overline{P}}{\varphi_c P_n} + \frac{\overline{M_x}}{\varphi_b M_{nx}} \leq 1.0 \qquad (2)$$

Where, $\overline{P}$ and $\overline{M_x}$ are required strengths, M_{nx} is the nominal flexural strength, and φ_b is the bending resistance factor. The Direct Strength Method (DSM) was used to calculate the nominal strengths. The critical elastic local and distortional buckling for both axial load and moment were determined using the signature curves obtained from section 5. Table 6 shows comparison of DSM with experimental results.

Table 6: Comparison of test results with AISI S100-16 prediction

Test Name	Bearing Condition	P_{max}	AISI S100 Capacity		P_{max}/P_n
			P_n	ϕP_n	
		kips (kN)	kips (kN)	kips (kN)	kips/kips (kN/kN)
600S16254F	Rigid	30.64 (136.28)	30.4 (135.1)	25.8 (114.8)	1.01
600S16254C	Full bearing	30.66 (136.39)	30.4 (135.1)	25.8 (114.8)	1.01
600S16254E1	1" to edge	27.67 (123.07)	30.4 (135.1)	25.8 (114.8)	0.91
600S16254E05	0.5" to edge	28.63 (127.33)	30.4 (135.1)	25.8 (114.8)	0.94
600S16254E0125	0.125" to edge	26.44 (117.61)	30.4 (135.1)	25.8 (114.8)	0.87
600S16254E	at the edge	25.97 (115.51)	30.4 (135.1)	25.8 (114.8)	0.86
600S16254O05	0.5" overhang	24.17 (107.52)	29.6 (131.7)	25.2 (111.9)	0.82
600S16254O1	1" overhang	20.03 (89.09)	28.7 (127.5)	24.4 (108.5)	0.70
600S30054E	at the edge	25.62 (113.94)	35.9 (159.5)	30.5 (135.6)	0.71
600S30054O05	0.5" overhang	21.05 (93.65)	35.5 (158.0)	30.2 (134.3)	0.59
600S30054O1	1" overhang	16.73 (74.44)	35.2 (156.4)	29.9 (133.0)	0.48

As it can be seen in Table 6, the DSM prediction is so close to the test results for both rigid and full bearing conditions. However, as the system get closer to the edge, the prediction becomes more far than the test results. For instance, for the 600S162-54 stud assembly at the edge, the predicted axial capacity is almost 17% larger than the corresponding amount in the experiments. And this amount for 1 inch (25.4 mm) overhang is almost 22%. This magnitude for the larger section is more severe and is almost 40% and 110% for at the edge and 1 inch (25.4 mm) overhang conditions respectively. It represents the wall assemblies which are placed close to the edge and are designed by the AISI S100 may have a smaller cross section than what is required. As a result, lack of a factor including the impact of non-uniform bearing conditions is felt.

7. Conclusions
Placing the wall assemblies near to the edge of concrete slab or even placing a part of them outside of the slab (overhang) is common in construction. In this research study, the impact of bearing condition on the axial behavior of two series of stud assemblies including 600S162-54 and 600S300-54 was explored. In total 11 test were done, and it was concluded in the full bearing condition (when the system is placed at the middle of concrete slab or there is enough distance to the edge), the slab can keep the stress distribution uniform; however, as the assembly get closer to the edge or overhang, the impact of non-uniform bearing condition on the axial capacity and the stiffness is boosted, which shows the axial strengths and stiffnesses are detrimental to non-uniform stress distribution. As an example, when the 600S162-54 assembly was placed at the edge or when it has one inch (25.4 mm) overhang, the axial peak load was decreased almost 15% and 35% respectively in comparison with rigid bearing condition; this can be a considerable decrease for designers. Since, there is not any guidance in AISI specifications herein, the test results were compared with axial strengths predicted by AISI S100-16. This comparison indicates the AISI predication is only match experimental results of rigid and full bearing conditions. Therefore, the AISI considers an overestimated axial strength for the members with non-uniform bearing conditions. Developing a design guide considering the impact of non-uniform bearing conditions is necessary, and it is recommended the impact of the investigated variables be taken into account in CFS wall assemblies behavior.

Future Work

The experiments will be expanded to fully encapsulate the experimental text matrix (Table 1) by performing experiments of 33 (0.84 mm) and 97 (2.46 mm) mil stud assemblies. Once the experimental results have been validated, the detailed Finite Element Analysis (FEM) model of the stud assemblies and concrete slabs as a system will be developed in ABAQUS to accurately predict not only the response of the stud assembly but also the contact behavior with the concrete slab along with the potential edge cracking and/or crushing of concrete slab itself. The detailed nonlinear FEA modeling aligns with the experimental effort and the necessity of a more extensive parametric study, and the parametric studies will be conducted with experimental variables not able to be tested for the developments of design provisions.

Acknowledgment

References

Joorabchian, A., Li, Z., and Peterman, K.D. (2018). "The Impact of Bearing Conditions on the Behavior of Cold- Formed Steel Stud Assemblies." *Proc. of International Specially Conference on Cold-Formed Steel Structures*, St. Louis, Missouri.

Peterman, K.D., and Schafer, B.W. (2014). "Sheated Cold-Formed Steed Studs under Axial and Lateral Load." *Journal of Construction Steel Research* 140(10): 1–12.

Vieira, L.C.M., Shifferaw, Y., and Schafer, B.W. (2011). "Experiments on Sheathed Cold-Formed Steel Studs in Compression." *Journal of Constructional Steel Research* 67(10): 1554–66.

AISI S100 (2016), North America Specification for the Desighn of Cold- Formed Steel Structures, American Iron and Steel Institude, Washington, D.C.

AISI S240 (2015), North America Standard for Cold-Formed Steel Structural Framing, American Iron and Steel Institute, Washington, D.C.

Vieira, L.C.M., and Schafer, B.W. (2011). "Behavior and Design of Sheathed Cold-Formed Steel Stud Walls under Compression." (*Ph.D. Thesis)*, The John Hopkins University.

Georgieva, I., Schueremans, L., and Pyl, L. (2012). "Composed Columns from Cold-Formed Steel Z-Profiles: Experiments and Code-Based Predictions of the Overall Compression Capacity." *Engineering Structures* 37: 125–34.

Li, Yuanqi, Li, Yinglei, Wang, S., and Shen, Z., (2014). "Ultimate Load-Carrying Capacity of Cold-Formed Thin-Walled Columns with Built-up Box and I Section under Axial Compression." *Thin-Walled Structures* 79: 202–17.

Jihong, Y., Feng, R., Chen, W., and Liu, W. (2016). "Behavior of Cold-Formed Steel Wall Stud with Sheathing Subjected to Compression." *Journal of Constructional Steel Research* 116: 79–91.

Xiangbin, L., and Zhou, T. (2017). "Research on Axial Compression Behavior of Cold-Formed Triple-Lambs Built-up Open T-Section Columns." *Journal of Constructional Steel Research* 134: 102–13.

Fangfang, L., Wu, H., Wang, R., and Zhou, T. (2017). "Compression Test and Analysis of Multi-Limbs Built-up Cold-Formed Steel Stub Columns." *Journal of Constructional Steel Research* 128: 405–15.

Fratamico, D.C., Torabian S., Rasmussen, K.J.R., and Schafer, B.W. (2016). "Experimental Studies on the Composite Action in Wood-Sheathed and Screw-Fastened Built-up Cold-

Formed Steel Columns." *Proc. of the Annual Stability Conference Conference, Structural Stability Research Counsile, Orlando, FL.*

Bae, S., Belarbi, A., and LaBoube. R.A. (2006). "Bearing Strength of Slabs on Grade Supporting a Cold-Formed Steel Wall in Low-Rise Building." *Journal of Architectural Engineering* 12(1): 24–32.

ACI Committee 318 (2005). Building Code Requirements for Structural Concrete (ACI 318-05) and Commentary (ACI 318R-05). Farmington Hills, Mich.: American Concrete Institute.

Polyzois, D., and Fox, S. (2001). "Light Gauge Steel Engineers Association Inside." Newsletter for the Light Gauge Steel Engineering Association (now the Cold-Formed Steel Engineering Institute).

Abaqus 6.14-4 (2014). Simulia, Dassault Systems, Providence, RI.

Schafer, B.W., and Ádány, S. (2006). "Buckling Analysis of Cold-Formed Steel Members Using CUFSM: Conventional and Constrained Finite Strip Method." *Proc. of 18th International Specialty Conference on Cold-Formed Steel Structures, Orlando, FL.*

Li, Z., Schafer, B.W. (2010) "Buckling analysis of cold-formed steel members with general boundary conditions using CUFSM: conventional and constrained finite strip methods." *Proc. of International Specially Conference on Cold-Formed Steel Structures*, St. Louis, Missouri.

Joorabchian, A., and Peterman, K.D. (2018). "Using Photogrammetry-Based Imperfection Measurement Tools to Determine the Impact of Corner Radii Imperfection on Cold-Formed Steel Member Strength." *Proc. of the Annual Stability Conference*, Structural Stability Research Counsile, Baltimore, Maryland.